

## Arsenic immobilization in anaerobic soils by the application of by-product iron materials obtained from the casting industry

メタデータ	言語: English 出版者: 公開日: 2019-09-27 キーワード (Ja): キーワード (En): Anaerobic soil, arsenic immobilization, by-product iron, phosphorus, silicon 作成者: 須田, 碧海, 山口, 紀子, 牧野, 知之 メールアドレス: 所属:
URL	<a href="https://repository.naro.go.jp/records/2762">https://repository.naro.go.jp/records/2762</a>

This work is licensed under a Creative Commons Attribution-NonCommercial-ShareAlike 3.0 International License.



1 Original article / Full-length paper

2  
3 Arsenic immobilization in anaerobic soils by the application of by-product  
4 iron materials obtained from the casting industry  
5

6  
7 Aomi Suda<sup>1)</sup>, Noriko Yamaguchi<sup>1)</sup>, Hayato Taniguchi<sup>2)</sup>, Tomoyuki Makino<sup>1)</sup>  
8

9 1) Institute for Agro-Environmental Sciences, NARO, 3-1-3, Kannondai, Tsukuba, Ibaraki 305-8604, Japan

10 2) Osaki Works, Sintokogio, Ltd., 1-1, Kado, Osaki-cho, Toyokawa,, Aichi, 442-8515, Japan  
11

12  
13 \* **Correspondence:**  
14

15 A. Suda, National Institute for Agro-Environmental Sciences, Kannondai 3-1-3, Tsukuba, Ibaraki 305-  
16 8604, Japan

17 E-mail: suda\_aomi@affrc.go.jp

18 Tel.: +81-29-838-8314

19 Fax: +81-29-838-8314  
20

21  
22 **Type of contribution:** Original article/Full-length paper  
23

24 **Division of manuscript:** Fertilizers and soil amendments  
25

26 **Running Title:** As immobilization using by-product Fe  
27  
28  
29  
30  
31  
32  
33  
34  
35  
36

37 **Abstract**

38 Reducing the arsenic (As) concentration in rice grains is of great interest from a human health  
39 perspective. Iron (Fe) materials immobilize As in soils, thereby effectively reducing the As  
40 concentration in rice grains. We investigated the effect of by-product Fe materials obtained from the  
41 casting industry on the As mobility in two soils (soil A and soil B) by a long-term (approximately 100  
42 days) flooded soil incubation experiment. The examined Fe materials were spent steel shot (SSS), fine  
43 spent casting sand containing steel shot (SCS), and two kinds of residual Fe materials from steel shot  
44 production (RIMs). Commercial Fe materials used to immobilize As (zero-valent Fe and ferrihydrite)  
45 were tested for comparison. The dissolved As in soil solution of controls for soil A and soil B reached  
46 approximately 100 and 800  $\mu\text{g L}^{-1}$ , respectively. The effect on As immobilization of all the by-product  
47 Fe materials increased with time and was comparable to or greater than that of commercial ferrihydrite,  
48 except for SCS. The additions of SSS and RIMs decreased by more than 90% of the dissolved As in  
49 soil A and decreased by more than 50% in soil B after 100 days incubation. Overall, the effect of the  
50 by-product Fe materials on the solubility of silicon and phosphorus was much less than that of the  
51 commercial Fe materials. Considering the cost advantage over commercial Fe materials, the Fe  
52 materials obtained from the casting industry as by-products are promising amendments for the  
53 immobilization of As in paddy soils.

54

55

56 ***Key Words: Anaerobic soil, Arsenic immobilization, By-product iron, Phosphorus, Silicon***

57

58

59

60

## 61 1. Introduction

62 Arsenic (As) species are hazardous chemicals that are ubiquitous in soils and plants. Since inorganic  
63 As species have greater toxicity than methylated species (Jain and Ali 2000), we need a strategy to  
64 decrease the concentration of inorganic As in foods. An important source of inorganic As for the Asian  
65 population is rice. For example, approximately 60% of the total intake of inorganic As by the average  
66 Japanese population was estimated to originate from rice (Oguri *et al.* 2014). In recent years, the Codex  
67 Alimentarius Commission adopted maximum permitted concentrations for inorganic As in polished  
68 and husked rice of 0.2 mg kg<sup>-1</sup> and 0.35 mg kg<sup>-1</sup>, respectively (Codex 2014; Codex 2016). Calculated  
69 from an investigation in Japan, approximately 2% of polished rice and 6% of brown rice grains  
70 produced in 2012 contained inorganic As levels exceeding 0.20 mg kg<sup>-1</sup> and 0.35 mg kg<sup>-1</sup>, respectively  
71 (MAFF 2014). Therefore, agronomic management practices to attenuate the uptake of inorganic As in  
72 rice grains must be established.

73 Honma *et al.* (2016a) showed that the As concentration in rice grains was positively correlated  
74 with the dissolved As concentration in soils. Since rice plants absorb As from the soil solution,  
75 restricting As dissolution from soil to decrease As uptake by rice is an effective strategy. Rice  
76 cultivation under aerobic (i.e., oxidative, water-saving) conditions decreases the As load in rice grains  
77 (Xu *et al.* 2009) because the As dissolution from soils decreases under aerobic conditions. However,  
78 aerobic cultivation results in the undesired accumulation of another harmful element, cadmium (Cd),  
79 in rice grains (Arao *et al.* 2009).

80 Another strategy for decreasing As dissolution from soils is the application of amendments to  
81 immobilize As in soils. Many studies reported that iron (Fe) materials such as Fe oxides (including  
82 hydroxides and oxyhydroxides) and zero-valent iron (ZVI) successfully immobilize As in soils  
83 (Kumpiene *et al.* 2008). Although most of the studies on As immobilization using amendments focused  
84 on polluted soils under aerobic conditions, some studies investigated the effect of Fe materials on As

85 mobility in non-polluted anaerobic soils, which are typical of Japanese paddy fields (Makino *et al.*  
86 2016; Suda *et al.* 2016). Makino *et al.* (2016) showed that the combination of flooded cultivation and  
87 the application of Fe materials was an effective measure to keep both As and Cd in rice grains at low  
88 concentrations. Honma *et al.* (2016b) also demonstrated that commercially available converter furnace  
89 slag and Fe hydroxide decreased As and Cd uptake, respectively, by rice plants grown on paddy fields.  
90 However, the high cost of Fe materials would limit their agricultural use.

91 Less-expensive Fe materials can be supplied by the casting industry from the use and production  
92 of steel shot. After the use of the steel shot, large amounts of spent steel shot (SSS) and fine spent  
93 casting sand (SCS) collected with dust collectors are produced. Residual iron materials (RIMs), which  
94 contain substantial amounts of Fe materials, are formed in the process of steel shot production. These  
95 by-product Fe materials could be sold for agricultural use at low prices. Some reports showed that the  
96 application of steel shot was effective at immobilizing As in contaminated soils under aerobic  
97 conditions (Boisson *et al.* 1999; Mench *et al.* 2003).

98 Another concern regarding the agricultural use of Fe materials is the possible decrease in silicon  
99 (Si) and phosphorus (P) availability because both ZVI and Fe oxides remove these elements from  
100 solution (Jordan *et al.* 2007; Zhu *et al.* 2011; Su *et al.* 2001). These elements are useful or essential  
101 for the growth of rice plants and affect As uptake by rice because rice plants take up arsenite via the  
102 silicate transport pathway (Ma *et al.* 2008) and arsenate via phosphate-arsenate co-transporters  
103 (Meharg 2004). Therefore, how the application of Fe materials affects dissolved Si and P in anaerobic  
104 soils must be understood.

105 The objectives of the present study were to investigate (1) the effect of by-product Fe materials  
106 from the casting industry on As mobility during long-term soil incubation under anaerobic conditions,  
107 (2) the effect of Fe materials on solubility of P and Si in soils, and (3) to discuss the availability of these  
108 materials as practical amendments to immobilize As in anaerobic paddy fields.

109

## 110 **2. Materials and methods**

### 111 **2.1 Soil samples**

112 Soil samples were collected from the surface layer of a paddy field in 2013 (Soil A) and from the  
113 surface layer of a fallow paddy field in 2010 (Soil B<sub>1</sub>) and in 2008 (Soil B<sub>2</sub>). These soil samples were  
114 air-dried and then screened through 2-mm mesh sieves. Selected soil properties, including soil pH,  
115 total carbon and nitrogen content, clay content, content of selectively extractable (with dithionite-  
116 citrate, oxalate and pyrophosphate) elements, and hydrochloric acid-extractable As content, were  
117 measured as described by Suda *et al.* (2015). The data on the selected soil properties are listed in Table  
118 1.

119

### 120 **2.2 Fe materials**

121 Fe materials from the casting industry were obtained from Sintokogio, Ltd. (Nagoya, Aichi,  
122 Japan). SSS is a mixture of spent steel shots collected from several foundries after use and then  
123 magnetically screened. SCS is composed of fine particles of spent casting sand with a small amount  
124 of steel shot. It is collected using dust collectors at foundries after sand removal in casting production.  
125 RIM-1 and RIM-2 are residual Fe materials of steel shot production. RIM-1 was obtained under wet  
126 conditions and was therefore dried at 30°C for several days. RIM-2 was collected using dust collectors  
127 at a steel shot production factory. Two types of commercial Fe materials, ZVI powder (cZVI) (Kobe  
128 Steel, Ltd., Tokyo, Japan) and ferrihydrite-based powder (cFH) (Ishihara Sangyo Kaisha, Ltd., Osaka,  
129 Japan) were used for comparison. Both cZVI and cFH are commercially supplied as amendments to  
130 immobilize As and heavy metals in soils. All the Fe materials were screened using 1-mm mesh sieves  
131 before use.

132 These Fe materials were digested with aqua-regia on a heating block, and the residue was

133 dissolved with hydrofluoric acid in a tightly sealed polypropylene tube at room temperature. Saturated  
134 boric acid was added to the tube to dissolve possible insoluble fluorides. The digested solution was  
135 used to quantify Fe, Si, Mn and P in the Fe materials. The Fe materials were also digested with an acid  
136 mixture (nitric acid:hydrochloric acid, 1:1) on a heating block to analyze the pseudo-total As in the Fe  
137 materials. The concentrations of elements in the digested solution were determined by inductively  
138 coupled plasma–optical emission spectrometry (ICP-OES; Vista-Pro, Agilent, California, USA) after  
139 dilution with ultra-pure water.

140 X-ray diffraction (XRD) analysis was carried out to clarify the mineral composition of the Fe  
141 materials. The Fe materials were passed through 212- $\mu\text{m}$  mesh sieves after gentle grinding with an  
142 aluminum mortar if necessary and possible. Since most of the SSS particles were  $>212\ \mu\text{m}$  and too  
143 hard to be crushed, both non-sieved ( $<1\ \text{mm}$ ) and sieved ( $<212\ \mu\text{m}$ ) fractions were analyzed by XRD.  
144 We adopted such a relatively large particle size to minimize the transformations of Fe minerals [e.g.,  
145 Fe(II) oxidation] during long-term grinding. The Fe in SCS was condensed using a magnet because of  
146 the low Fe content of this material. XRD patterns were obtained under the following conditions: X-  
147 ray diffractometer, Rint2200 (Rigaku, Tokyo, Japan); Cu  $K\alpha$ , Ni filter; 40 kV, 40 mA; slit system,  $1^\circ$ –  
148  $1^\circ$ –0.15 mm. The scanned range was 20 to  $85^\circ 2\theta$  in  $0.02^\circ$  steps, with a scanning rate of  $1^\circ$  per min.

149 The particle-size distributions of the Fe materials were evaluated by sieving through mesh sizes  
150 of 0.850, 0.710, 0.600, 0.500, 0.425, 0.355, 0.300, 0.250, 0.212, 0.180, 0.150, 0.125, 0.106, 0.075, and  
151 0.045 mm.

152

### 153 ***2.3. Anaerobic incubation of soil and quantification of elements in the soil solution***

154 Soils A and B<sub>1</sub> were incubated under anaerobic conditions to clarify the effects of the Fe materials on  
155 the concentrations of As, Si and P in the soil solution. An air-dried soil sample (10 g, oven-dried basis)  
156 and 100 mg of each Fe material were mixed with 30 mL of ultra-pure water in a glass vial. A similar

157 sample without any Fe material was also prepared as a control. After nitrogen gas (N<sub>2</sub>) bubbling for 2  
158 min, the vial was capped with a butyl rubber cap and then tightly sealed with an aluminum cap. The  
159 capped vial was shaken by hand and then incubated at 30 °C for approximately 20, 60 and 100 days.  
160 The precise incubation periods were 21, 60, and 102 days for soil A and 20, 60, and 99 days for soil  
161 B<sub>1</sub>, respectively. The vial was shaken by hand with at 1-2-day intervals. These incubation experiments  
162 were performed in triplicate.

163 After incubation, the soil solution was collected by a syringe connected to a needle (NN-2360C,  
164 Terumo Corporation, Tokyo, Japan) with a 0.2-μm filter (DG2M-330, Spectrum Laboratories, Inc.,  
165 CA, USA). The sampling unit was purged with N<sub>2</sub> before use. Approximately 4.5 mL of filtrate was  
166 immediately mixed with 0.5 mL of 1.6 mol L<sup>-1</sup> nitric acid to prevent Fe-hydroxide precipitation. The  
167 acidified filtrate was diluted, and the Fe, Si, P and As concentrations in the diluted solution were  
168 measured using ICP-OES and inductively coupled plasma–mass spectrometry (ICP–MS; Elan DRC-  
169 e, PerkinElmer, Waltham, MA, USA).

170 The efficacy of the Fe materials in immobilizing As, Si and P in soils at each sampling time was  
171 evaluated as the percent decrease in the dissolved elements compared with those in the control soils,  
172 as defined by the following equation:

$$173 \quad \text{Percent decrease in dissolved element} = \frac{(CE_{cont} - CE_{Fe})}{CE_{cont}} \times 100 (\%) \quad (Eq. 1)$$

174 where (CE<sub>Fe</sub>) and (CE<sub>cont</sub>) are the concentrations of the element in the soil solution incubated with and  
175 without the Fe material, respectively.

176

#### 177 **2.4. Speciation of As in the soil solid phase**

178 Soil B<sub>2</sub> with or without cZVI was anaerobically incubated for 100 days in triplicate as described  
179 in the former paragraph. The three incubated soil samples of each treatment were mixed under a N<sub>2</sub>  
180 atmosphere, and the mixture was then centrifuged to separate the soil solution from the solids. After

181 removing the soil solution, an aliquot of wet soil paste was packed into a polyethylene bag and kept  
182 frozen until analysis.

183 As K-edge (11867 eV) X-ray absorption near-edge structure (XANES) spectra were obtained on  
184 BL12C of the photon factory, KEK, and on BL5S1 of the Aichi Synchrotron Radiation Center.  
185 Reference materials, Na<sub>2</sub>AsO<sub>3</sub> [As(III)], NaHAsO<sub>4</sub> [As(V)], orpiment (As<sub>2</sub>S<sub>3</sub>), and arsenopyrite  
186 (FeAsS, Francisco I. Madero Mine, Mexico, N's Mineral) were diluted by boron nitride, and the  
187 XANES spectra were collected in the transmission mode. The XANES spectra of the incubated soil  
188 pastes were collected in the fluorescence detection mode using a 19-element Ge semiconductor  
189 detector. The relative proportion of As species in the soil solid phases were calculated by linear  
190 combination fitting (LCF) of the XANES spectra with the reference materials. The fitting range was  
191 11855 to 11885 eV. Athena in the Demeter 0.9.25 program package was used for XANES data analysis.

192

### 193 ***2.5. Statistical analysis***

194 The dissolved element concentrations were subjected to two-way analysis of variance (ANOVA).  
195 Based on the output from ANOVA, multiple comparisons were made using Tukey's test at a 0.05  
196 probability level. All statistical analyses were performed using Microsoft Excel and R software  
197 (version 3.1.1).

198

## 199 **3. Results**

### 200 ***3.1. Properties of Fe materials***

201 Table 2 shows the concentrations of major elements and kinds of XRD-detectable minerals in the  
202 Fe materials. The concentrations of Fe and Si followed orders of cZVI > SSS >> RIM-2 > RIM-1 >  
203 cFH >>> SCS and SCS >>> RIM-1 = RIM-2 = SSS > cZVI = cFH, respectively. The As and P  
204 concentrations ranged from 3.27 to 76.8 mg kg<sup>-1</sup> and from 102 to 639 mg kg<sup>-1</sup>, respectively. The major

205 Fe minerals in each Fe material were Fe(0) for SSS, SCS and cZVI; wüstite and magnetite/maghemite  
206 for RIM-1 and RIM-2; and ferrihydrite for cFH (Table 2, Fig. S1). Since steel shot-like spherical  
207 particles were observed in the <212 µm fraction that accounted for approximately 12% of total weight,  
208 the Fe(0) in RIM-2 (Fig. S1, f) should be derived from fine steel particles. All Fe materials were mainly  
209 composed of Fe minerals except for SCS, which was dominated by quartz. Quartz in SSS and SCS  
210 should originate from casting sand.

211 The particle distributions of the Fe materials are shown in Figure S2. RIM-1, cFH and cZVI  
212 contained substantial amounts of particles in their finest fractions (less than 0.045 µm). The coarsest  
213 Fe material was SSS. More than 30 wt% of the SSS particles did not pass through a 0.5 mm mesh  
214 sieve.

215

### 216 ***3.2. Effect of Fe materials on As dissolution***

217 After soil incubation without Fe materials, the As concentrations in solution were 21.9 (day 20),  
218 108 (day 60) and 98.2 (day 100) µg L<sup>-1</sup> for soil A and 367, 649 and 817 µg L<sup>-1</sup> for soil B<sub>1</sub>, respectively  
219 (Table 3). Two-way ANOVA demonstrated the significant effects ( $P < 0.001$ ) of the Fe material, the  
220 incubation time, and the interaction between the Fe material and incubation time on the dissolved As  
221 concentration. Except for day 20 in soil A, the percent decrease in dissolved As in both soils decreased  
222 in the following order at all incubation times: cZVI > SSS > RIM-2 = RIM-1 > SCS (Fig. 1). The  
223 effect of these Fe materials on As immobilization increased over time, while that of cFH remained at  
224 a similar level or gradually decreased.

225

### 226 ***3.3 As speciation in the soil solid phase with the addition of ZVI***

227 Figure 2 shows the As K-edge XANES spectra of soil B<sub>2</sub> incubated with and without cZVI under  
228 anaerobic conditions. Without cZVI, the major As species in the soil solid phase was As(III), and the

229 percentages of As<sub>2</sub>S<sub>3</sub>-like species, As(III) and As(V) were 10, 72 and 18%, respectively. The XANES  
230 spectra of soil incubated with cZVI had a distinct shoulder at approximately 11870 eV, which was not  
231 apparent in the spectrum of the soil incubated without cZVI. This shoulder peak indicated the presence  
232 of As associated with S. The percentages of FeAsS-like species, As<sub>2</sub>S<sub>3</sub>-like species, As(III) and As(V)  
233 in the soil incubated with cZVI were 28, 15, 20 and 37%, respectively. Thus, the addition of cZVI  
234 decreased the percentage of As(III) while increasing the percentages of As(V) and As associated with  
235 S in the soil solid phase. Since we used synthesized or natural minerals as reference materials for As  
236 associated with S in the LCF, the mineral crystallinity and exact elemental composition may be  
237 different from those of As associated with S in the incubated soil. In addition, the LCF results represent  
238 the presence of As species which have similar local coordinations with As<sub>2</sub>S<sub>3</sub> and FeAsS, and not  
239 necessary represent the presence of As<sub>2</sub>S<sub>3</sub> and FeAsS exactly. Nonetheless, an increased contribution  
240 of As species associated with S from the addition of cZVI was clearly observed in the XANES spectra.  
241

#### 242 ***3.4. Effect of Fe materials on the dissolved Si, P and Fe concentrations***

243 The concentration of Si dissolved from soils increased over time regardless of the addition of Fe  
244 materials (Table 3). The Si concentrations were 8.02 (day 20), 11.3 (day 60) and 12.5 mg L<sup>-1</sup> (day  
245 100) in soil A and 11.1, 12.0, and 13.2 mg L<sup>-1</sup> in soil B<sub>1</sub>, respectively, without any Fe materials. Two-  
246 way ANOVA revealed the significant effects of the Fe material, the incubation time, and the interaction  
247 between the Fe material and incubation time on the dissolved Si ( $P < 0.001$ ) (Table 3). The impact of  
248 Fe materials on the dissolved Si concentration in soil A was slightly larger than that in soil B. For soil  
249 A, the additions of SSS, SCS, and especially RIM-1 and RIM-2 caused significant increases in  
250 dissolved Si (except for SSS at day 100). On the other hand, the applications of cFH and cZVI caused  
251 statistically significant decreases in dissolved Si (Tukey test,  $P = 0.05$ ) in all cases.

252 The dissolved P in soils increased with the incubation time (Table 3). The P dissolved from soils

253 without Fe materials was 1.15 (day 20), 2.01 (day 60) and 2.24 mg L<sup>-1</sup> (day 100) in soil A and 0.480,  
254 0.597, and 0.667 mg L<sup>-1</sup> in soil B<sub>1</sub>, respectively. Significant effects of the Fe material, the incubation  
255 time, and their interaction on the dissolved P concentration were demonstrated by two-way ANOVA  
256 ( $P < 0.001$ ). The dissolved P significantly decreased due to the applications of cFH and cZVI, except  
257 in soil A with cZVI at day 20. The additions of by-product Fe materials tended to decrease the  
258 dissolved P in soil B<sub>1</sub>, although the change was small and not statistically significant (Tukey test,  $P =$   
259 0.05) in most cases.

260 The concentration of Fe dissolved from soils without Fe materials increased over time, although  
261 the change was not remarkable compared to the change in As (Table S1). The dissolved Fe content  
262 was 49.8 (day 20), 97.6 (day 60) and 109 mg L<sup>-1</sup> (day 100) in soil A and 85.0, 97.5, and 104 mg L<sup>-1</sup>  
263 in soil B<sub>1</sub>, respectively (Table S1). The additions of Fe materials did not increase the dissolved Fe in  
264 most cases. SSS and cZVI increased the dissolved Fe at day 20 in soil A, whereas cZVI (soil A and  
265 B<sub>1</sub>) and cFH (soil B<sub>1</sub>) substantially decreased the dissolved Fe.

266

## 267 **4. Discussion**

### 268 **4.1. As immobilization**

#### 269 **4.1.1. SSS, SCS and cZVI**

270 SSS and cZVI, which are composed mainly of ZVI, effectively decreased the As dissolution from soils  
271 under the anaerobic conditions (Table 3, Fig. 1). The larger effect of cZVI on As immobilization  
272 compared to that of SSS was probably attributable to the smaller particle size of cZVI (Fig. S2). SCS  
273 decreased As dissolution less than SSS and cZVI did, reflecting the low content of Fe in SCS (Table  
274 2). The percent decrease in dissolved As with the addition of these materials increased as time  
275 proceeded (Fig. 1a and b). These results indicated that the Fe materials can immobilize As over a long  
276 period even under anaerobic conditions.

277 Corrosion products of ZVI, mainly Fe oxides, are known to sorb As under aerobic conditions.  
278 However, development of a corrosion layer of ZVI and the subsequent removal of As from solution is  
279 limited under anaerobic conditions compared with aerobic conditions (Klas and Kirk 2013). Therefore,  
280 the sorption of As onto the corrosion products of ZVI might not be a major mechanism restricting As  
281 dissolution from soils under anaerobic conditions as in the present study.

282 The XANES spectra indicated that cZVI addition substantially increased the formation of As  
283 species associated with S under anaerobic conditions (Fig. 2). Arsenopyrite was not observed in the  
284 control soil but accounted for 28% of the total As in the soil incubated with cZVI. Therefore, As  
285 precipitation as sulfides, especially as FeAsS-like species, might contribute to the As immobilization  
286 caused by the application of cZVI, SSS and SCS. Hydrogen gas generation accompanying water  
287 reduction by ZVI promotes microbial sulfate reduction (Gu *et al.* 1999) and possibly induces the  
288 subsequent formation of insoluble sulfides of As and Fe.

289 The percentage of As(V) in the soil incubated with cZVI was substantially higher than that in the  
290 control soil. Since the affinity of As(V) for soil solid phase is greater than that of As(III) (Takahashi *et*  
291 *al.* 2003), As(III) oxidation is expected to decrease the As mobility in soils. Considering the strictly  
292 anaerobic conditions of the incubation experiment, As(III) oxidation by dissolved oxygen and Fenton's  
293 reaction unlikely occurred substantially. Instead, As(III) oxidation at the Fe oxide shell on ZVI surface  
294 (Yan *et al.* 2010) might be an explanation. Yan *et al.* (2012) inferred that the As(III) oxidation by ZVI  
295 caused via an Fe oxide-Fe(II)-As(III) ternary complex, which was an As(III) oxidation mechanism in  
296 anaerobic Fe oxide-Fe(II) systems previously suggested by Amstaetter *et al.* (2010). Although we have  
297 no evidence, the reaction should not be ruled out as a candidate mechanism for the As immobilization  
298 in soils anaerobically incubated with cZVI, SSS and SCS.

299

300 **4.1.2. RIM-1 and RIM-2**

301 The additions of RIM-1 and RIM-2 immobilized As in soils, although this immobilization was  
302 less effective than that by SSS and cZVI. Since these RIMs contained magnetite/maghemite and a  
303 small amount of hematite (only RIM-1), the sorption of As on these Fe oxides (Giménez *et al.* 2007)  
304 would contribute to As immobilization. However, As removal by wüstite, which is a major Fe mineral  
305 in these Fe materials, is limited under low-dissolved-oxygen conditions (Mishra and Farrell 2005).  
306 Interestingly, the percent decrease in dissolved As increased with time in both soils (Fig. 1). Although  
307 RIM-2 contained Fe(0), As immobilization by Fe(0) would be limited due to the small amount of Fe(0).  
308 Arsenic(III) was oxidized to As(V) at the surface of Fe oxides, including magnetite and hematite, even  
309 under anaerobic conditions (Yan *et al.* 2010). Since the oxidation is considered to occur via reactive  
310 Fe(III)-Fe(II) species and/or secondary Fe(II)/Fe(III) mineral phases (Amstaetter *et al.* 2010), it might  
311 be facilitated by increase of Fe(II) dissolution and secondary Fe precipitation as time proceeded.  
312 However, there is no experimental evidence to support this hypothesis. Further studies are needed to  
313 investigate Fe and As speciation in order to propose mechanisms for As immobilization under  
314 anaerobic soil conditions amended with Fe materials containing Fe(II) and Fe(II)/Fe(III) minerals.

#### 315 **4.1.3. cFH**

316 The major component of cFH, ferrihydrite, has a large specific surface area (100-700 m<sup>2</sup> g<sup>-1</sup>;  
317 Cornel and Schwertmann 2003) and therefore adsorbs large amounts of oxyanions such as arsenate  
318 and phosphate. The high specific surface area expected based on the small particle size (Fig. S2) might  
319 explain high efficiency of cFH in As immobilization. Unlike other Fe materials, the percent decrease  
320 in dissolved As remained at a similar level (Soil A) or gradually decreased (Soil B) over time. A similar  
321 trend was observed in a previous study (Suda *et al.* 2015) showing that As immobilization by synthetic  
322 ferrihydrite decreased with time under similar incubation conditions. Although the reductive  
323 transformation of ferrihydrite to magnetite temporarily increases As retention (Kocar *et al.* 2006),  
324 prolonged anaerobic conditions cause As release that results from diminishing binding sites on the

325 surface of Fe oxides (Tufano and Fendorf 2008). Furthermore, As sorption onto Fe oxides would be  
326 inhibited by co-existing substances, such as silicate, phosphate, carbonate species, and dissolved  
327 organic matter (Jain and Loeppert 2000; Swedlund and Webster 1999; Brechbühl *et al.* 2012; Grafe *et*  
328 *al.* 2002). In the present study, the concentrations of carbonate and dissolved organic carbon were not  
329 measured, but Table S1 shows a decreasing trend in the dissolved Si/As and P/As ratios in the control  
330 soils as time proceeded. Therefore, the competition for adsorption sites on the cFH surface with co-  
331 existing dissolved silicate and phosphate would not be a major cause of the decrease in As  
332 immobilization efficiency with the addition of cFH.

333

#### 334 **4.2. Si and P dissolution**

335 The impact of Fe materials on the dissolved Si concentration in soil A was greater than that on soil B.  
336 In soil A, the additions of RIM-1 and RIM-2 increased the dissolved Si most significantly, although  
337 the Si content in SCS was approximately six times greater than those in RIM-1 and RIM-2. This result  
338 reflects the difference in Si minerals among these Fe materials. RIM-1 and RIM-2 contain amorphous  
339 (i.e., not XRD-detectable) Si, whereas SCS contains quartz, which is hardly soluble in soil solution  
340 (Table 4). Since As(III) is transported by the same pathways as Si (Ma *et al.* 2008), dissolved Si inhibits  
341 the uptake of As by rice plants (Li *et al.* 2009). Therefore, RIM-1 and RIM-2 potentially decrease As  
342 uptake in rice plants by supplying dissolved Si. On the other hand, cFH resulted in the largest percent  
343 decrease in dissolved Si among all the Fe materials, which reached 24% in soil A and 18% in soil B<sub>1</sub>,  
344 because of the Si sorption onto ferrihydrite (Swedlund and Webster 1999).

345 Figure 3 shows the relationships between the percent decrease in dissolved As and that in  
346 dissolved P in soil B<sub>1</sub> incubated with Fe materials. The regression line for the by-product Fe materials  
347 indicates that the percent decrease in dissolved P was positively correlated with that in dissolved As  
348 ( $r = -0.723$ ,  $P < 0.001$ ). This result indicated that As immobilization was accompanied by a decrease

349 in P solubility. However, the percent decrease in dissolved As was much greater than the percent  
350 decrease in dissolved P, except in the case of cFH. The considerable difference in the ratio of the  
351 percent decrease in dissolved As to that in dissolved P between cFH and the other Fe materials might  
352 reflect the presence of different mechanisms of As immobilization between these materials, i.e., the  
353 adsorption of As onto the surface hydroxyl groups of Fe oxides was not main mechanism of As  
354 immobilization by the Fe materials, other than cFH. The same analysis was not carried out for soil A  
355 because the percent decrease in dissolved As at day 60 and day 100 reached nearly 100% in most cases.  
356 Overall, the by-product Fe materials did not substantially decrease dissolved P in soil A as the  
357 commercial Fe materials did, except for SSS at day 100 (Table 3).

358

#### 359 ***4.3. Potential of the by-product Fe materials to immobilize As in paddy soils***

360 Due to their complex compositions, determining the precise mechanisms of As immobilization  
361 by the application of by-product Fe materials is difficult. However, the present study clearly showed  
362 the high ability of by-product Fe materials, namely SSS, RIM-1 and RIM-2, to immobilize As in  
363 flooded anaerobic soils. Although cZVI more effectively restricted As dissolution from soils, the  
364 application of by-product Fe materials is more cost-effective than the application of cZVI. Furthermore,  
365 the application of by-product Fe materials did not cause significant decreases in Si and P dissolution  
366 compared with cFH. (Table 3, Fig. 2). This is desirable for both plant growth and the inhibition of As  
367 uptake by these elements. Therefore, we concluded that these by-product Fe materials are promising  
368 amendments for As immobilization in paddy soils, at least on a single-use basis.

369 In most cases, the dissolved Fe in soils incubated with the Fe materials did not substantially  
370 increase (Table S1). This result indicated that the Fe materials were relatively stable under anaerobic  
371 conditions. However, we cannot rule out the possibility that excess the Fe(II) derived from Fe materials  
372 adsorbed onto the soil solid phase and/or precipitated as secondary Fe minerals such as siderite

373 (Yamaguchi *et al.* 2011). In either case, the applied Fe materials eventually dissolve as Fe(II), followed  
374 by reoxidization to Fe(III) by dissolved oxygen. Therefore, regardless of their mineral composition,  
375 the applied Fe materials will ultimately dissolve, but their effect will persist to some extent due to the  
376 increase in Fe oxides in the applied soils. The Fe materials applied to paddy soil are most likely altered  
377 after repeated cycles of anaerobic and aerobic conditions, but their resistance against dissolution in  
378 soil under paddy field conditions remains unclear. Long-term and field-scale experiments should be  
379 carried out to assess the time course of As mobility in soils with Fe materials before agricultural use.

380

### 381 **Acknowledgements**

382 We deeply appreciate the dedicated assistance of Mr. Taichi Hihara throughout the research. The  
383 authors also thank Dr. Toshiaki Ohkura (Institute for Agro-Environmental Sciences, NARO) for his  
384 support in using the X-ray diffractometer. We thank Dr. Tomohito Arao (Central Region Agricultural  
385 Research Center, NARO), Dr. Akira Kawasaki (Advanced Analysis Center, NARO), Dr. Koji Baba,  
386 Ken Nakamura (Institute for Agro-Environmental Sciences, NARO), and Mr. Satoshi Takamiya  
387 (Ministry of Agriculture, Forestry and Fisheries) for their useful suggestions and comments. The  
388 XANES measurements were performed with the approval of the High-Energy Accelerator Research  
389 Organization, KEK (Proposal No. 2011G016), and the Aichi Synchrotron Radiation Center (Proposal  
390 No. 201606072). The ICP-OES and ICP-MS measurements were carried out at the Advanced Analysis  
391 Center, NARO.

392 Main part of this work was supported by the Ministry of Agriculture, Forestry and Fisheries under  
393 a Grant-in-Aid for the research project for improving food safety and animal health As-210. Other  
394 aspects of this work were conducted under the collaborative research agreement between the Institute  
395 for Agro-Environmental Sciences, NARO, and Sintokogio Ltd.

396

397 **References**

- 398 Amstaetter K, Borch T, Larese-Casanova P, Kappler A 2010: Redox transformation of arsenic by  
399 Fe(II)-activated goethite ( $\alpha$ -FeOOH). *Environ. Sci. Technol.*, 44, 102–108.
- 400 Arao T, Kawasaki A, Baba K, Mori S, Matsumoto S 2009: Effects of water management on cadmium  
401 and arsenic accumulation and dimethylarsinic acid concentrations in Japanese rice. *Environ. Sci.*  
402 *Technol.*, 43, 9361–9367.
- 403 Boisson J, Mench M, Vangronsveld J, Ruttens A, Kopponen P, De Koe T 1999: Immobilization of  
404 trace metals and arsenic by different soil additives: Evaluation by means of chemical extractions.  
405 *Commun. Soil Sci. Plant Anal.*, 30, 365–387.
- 406 Brechbühl Y, Christl I, Elzinga EJ, Kretzschmar R 2012: Competitive sorption of carbonate and arsenic  
407 to hematite: combined ATR-FTIR and batch experiments. *J. Colloid Interface Sci.*, 377, 313–321.
- 408 Codex Alimentarius Commission. 2014: Thirty-Seventh Session CICG, Geneva; 2014 Jul 14–18.  
409 [http://www.fao.org/fao-who-codexalimentarius/sh-](http://www.fao.org/fao-who-codexalimentarius/sh-proxy/en/?lnk=1&url=https%253A%252F%252Fworkspace.fao.org%252Fsites%252Fcodex%252FMeetings%252FCX-701-37%252FREP14_CACe.pdf)  
410 [proxy/en/?lnk=1&url=https%253A%252F%252Fworkspace.fao.org%252Fsites%252Fcodex%252F](http://www.fao.org/fao-who-codexalimentarius/sh-proxy/en/?lnk=1&url=https%253A%252F%252Fworkspace.fao.org%252Fsites%252Fcodex%252FMeetings%252FCX-701-37%252FREP14_CACe.pdf)  
411 [Meetings%252FCX-701-37%252FREP14\\_CACe.pdf](http://www.fao.org/fao-who-codexalimentarius/sh-proxy/en/?lnk=1&url=https%253A%252F%252Fworkspace.fao.org%252Fsites%252Fcodex%252FMeetings%252FCX-701-37%252FREP14_CACe.pdf) (April, 2017)
- 412 Codex Alimentarius Commission. 2016: Thirty-Ninth Session CICG, Rome; 2016 27 June - 1 July.  
413 [http://www.fao.org/fao-who-codexalimentarius/sh-](http://www.fao.org/fao-who-codexalimentarius/sh-proxy/en/?lnk=1&url=https%253A%252F%252Fworkspace.fao.org%252Fsites%252Fcodex%252FMeetings%252FCX-701-39%252FREPORT%252FREP16_CACe.pdf)  
414 [proxy/en/?lnk=1&url=https%253A%252F%252Fworkspace.fao.org%252Fsites%252Fcodex%252F](http://www.fao.org/fao-who-codexalimentarius/sh-proxy/en/?lnk=1&url=https%253A%252F%252Fworkspace.fao.org%252Fsites%252Fcodex%252FMeetings%252FCX-701-39%252FREPORT%252FREP16_CACe.pdf)  
415 [Meetings%252FCX-701-39%252FREPORT%252FREP16\\_CACe.pdf](http://www.fao.org/fao-who-codexalimentarius/sh-proxy/en/?lnk=1&url=https%253A%252F%252Fworkspace.fao.org%252Fsites%252Fcodex%252FMeetings%252FCX-701-39%252FREPORT%252FREP16_CACe.pdf) (April, 2017)
- 416 Cornell RM, Schwertmann U 2003: Surface area and Porosity. In: *The Iron Oxides: Structure,*  
417 *Properties, Reactions, Occurrences and Uses*, pp. 87–102. Wiley-VCH: Weinheim.
- 418 Giménez J, Martínez M, de Pablo J, Rovira M, Duro L 2007: Arsenic sorption onto natural hematite,  
419 magnetite, and goethite. *J. Hazard. Mater.*, 141, 575–80.
- 420 Grafe M, Eick MJ, Grossl PR, Saunders AM 2002: Adsorption of arsenate and arsenite on ferrihydrite

421 in the presence and absence of dissolved organic carbon. *J. Environ. Qual.*, 31, 1115–1123.

422 Gu B, Phelps TJ, Liang L, Dickey MJ, Roh Y, Kinsall BL, Palumbo AV, Jacobs GK 1999:  
423 Biogeochemical dynamics in zero-valent iron columns: implication for permeable reactive barriers.  
424 *Environ. Sci. Technol.*, 33, 2170–2177.

425 Honma T, Ohba H, Kaneko A, Nakamura K, Makino T, Katou H 2016b: Effects of soil amendments  
426 on arsenic and cadmium uptake by rice plants (*Oryza sativa* L. cv. Koshihikari) under different  
427 water management practices. *Soil Sci. Plant Nutr.*, 62, 349–356.

428 Honma T, Ohba H, Kaneko-Kadokura A, Makino T, Nakamura K, Katou H 2016a: Optimal Soil Eh,  
429 pH, and Water Management for Simultaneously Minimizing Arsenic and Cadmium Concentrations  
430 in Rice Grains. *Environ. Sci. Technol.*, 50, 4178–4185.

431 Jain A, Loeppert R 2000: Effect of competing anions on the adsorption of arsenate and arsenite by  
432 ferrihydrite. *J. Environ. Qual.*, 29, 1422–1430.

433 Jain CK, Ali I 2000: Arsenic: Occurrence, toxicity and speciation techniques. *Water Res.*, 34, 4304–  
434 4312.

435 Jordan N, Marmier N, Lomenech C, Giffaut E, Ehrhardt JJ 2007: Sorption of silicates on goethite,  
436 hematite, and magnetite: Experiments and modelling. *J. Colloid Interface Sci.*, 312, 224–229.

437 Klas S, Kirk DW 2013: Advantages of low pH and limited oxygenation in arsenite removal from water  
438 by zero-valent iron. *J. Hazard. Mater.*, 252–253, 77–82.

439 Kocar BD, Herbel MJ, Tufano KJ, Fendorf S 2006: Contrasting effects of dissimilatory iron (III) and  
440 arsenic (V) reduction on arsenic retention and transport. *Environ. Sci. Technol.*, 40, 6715–6721.

441 Kumpiene J, Lagerkvist A, Maurice C 2008: Stabilization of As, Cr, Cu, Pb and Zn in soil using  
442 amendments—a review. *Waste Manag.*, 28, 215–225.

443 Li RY, Stroud JL, Ma JF, McGrath SP, Zhao FJ 2009: Mitigation of arsenic accumulation in rice with  
444 water management and silicon fertilization. *Environ. Sci. Technol.*, 43, 3778–3783.

445 Ma JF, Yamaji N, Mitani N, Xu X-Y, Su Y-H, McGrath SP, Zhao F-J 2008: Transporters of arsenite in  
446 rice and their role in arsenic accumulation in rice grain. Proc. Natl. Acad. Sci. U. S. A., 105, 9931–  
447 9935.

448 MAFF 2014: Survey of arsenic levels in brown rice and polished rice produced in Japan.  
449 <http://www.maff.go.jp/j/press/syouan/nouan/pdf/140221-01.pdf> (in Japanese, October, 2015)

450 Makino T, Nakamura K, Katou H, *et al.* 2016: Simultaneous decrease of arsenic and cadmium in rice  
451 (*Oryza sativa* L.) plants cultivated under submerged field conditions by the application of iron-  
452 bearing materials. Soil Sci. Plant Nutr., 62, 340–348.

453 Meharg AA 2004: Arsenic in rice-understanding a new disaster for South-East Asia. Trends Plant Sci.,  
454 9, 415–417.

455 Mench M, Bussière S, Boisson J, Castaing E, Vangronsveld J, Ruttens A, DeKoe T, Bleeker P,  
456 Assunção A, Manceau A 2003: Progress in remediation and revegetation of the barren Jales gold  
457 mine spoil after in situ treatments. Plant Soil, 249, 187–202.

458 Mishra D, Farrell J 2005: Evaluation of mixed valent iron oxides as reactive adsorbents for arsenic  
459 removal. Environ. Sci. Technol., 39, 9689–9694.

460 Oguri T, Yoshinaga J, Tao H, Nakazato T 2014: Inorganic arsenic in the Japanese diet: Daily intake  
461 and source. Arch. Environ. Contam. Toxicol., 66, 100–112.

462 Su C, Puls RW 2001: Arsenate and arsenite removal by zerovalent iron: Effects of phosphate, silicate,  
463 carbonate, borate, sulfate, chromate, molybdate, and nitrate, relative to chloride. Environ. Sci.  
464 Technol., 35, 4562–4568.

465 Suda A, Baba K, Akahane I, Makino T 2016: Use of water-treatment residue containing polysilicate-  
466 iron to stabilize arsenic in flooded soils and attenuate arsenic uptake by rice (*Oryza sativa* L.) plants.  
467 Soil Sci. Plant Nutr., 62, 111–116.

468 Suda A, Baba K, Yamaguchi N, Akahane I, Makino T 2015: The effects of soil amendments on arsenic

469 concentrations in soil solutions after long-term flooded incubation. *Soil Sci. Plant Nutr.*, 61, 592–  
470 602.

471 Swedlund PJ, Webster JG 1999: Adsorption and polymerization of silicic acid on ferrihydrite, and its  
472 effect on arsenic adsorption. *Water Res.*, 33, 3413–3422.

473 Takahashi Y, Ohtaku N, Mitsunobu S, Yuita K, Nomura M 2003: Determination of the As(III)/As(V)  
474 ratio in soil by X-ray absorption near-edge structure (XANES) and its application to the arsenic  
475 distribution between soil and water. *Anal. Sci.*, 19, 891–896.

476 Tufano KJ, Fendorf S 2008: Confounding impacts of iron reduction on arsenic retention. *Environ. Sci.*  
477 *Technol.*, 42, 4777–4783.

478 Xu XY, Mcgrath SP, Mehaarg AA, Zhao FJ 2009: Growing rice aerobically markedly decreases arsenic  
479 accumulation. *Environ. Sci. Technol.*, 43, 5574–5579.

480 Yamaguchi N, Nakamura T, Dong D, Takahashi Y, Amachi S, Makino T 2011: Arsenic release from  
481 flooded paddy soils is influenced by speciation, Eh, pH, and iron dissolution. *Chemosphere*, 83,  
482 925–932.

483 Yan W, Ramos MA V, Koel BE, Zhang WX 2010: Multi-tiered distribution of arsenic in iron  
484 nanoparticles: Observation of dual redox functionality enabled by a core shell structure. *Chem.*  
485 *Commun.*, 46, 6995–6997.

486 Yan W, Ramos MA V, Koel BE, Zhang WX 2012: As(III) sequestration by iron nanoparticles: Study  
487 of solid-phase redox transformations with X-ray photoelectron spectroscopy. *J. Phys. Chem. C*, 116,  
488 5303–5311.

489 Zhu J, Pigna M, Cozzolino V, Caporale AG, Violante A 2011: Sorption of arsenite and arsenate on  
490 ferrihydrite: Effect of organic and inorganic ligands. *J. Hazard. Mater.*, 189, 564–571.

491

492

## Table and Figure Legends

493

494

495 Fig. 1 Time course changes in the percent decrease in dissolved arsenic (As) in soil A (a) and soil B1  
496 (b) incubated with each Fe material. SSS, SCS, RIM, cFH and cZVI denote spent steel shot, fine spent  
497 casting sand, residual iron material of steel shot production, commercial ferrihydrite and commercial  
498 zero-valent iron, respectively. The percent decrease in dissolved As was calculated using Eq. 1.

499

500 Fig. 2 Arsenic K-edge XANES spectra of solid phases of (a) the control for soil B2 and (b) soil B2  
501 incubated with commercial zero-valent iron. Broken lines indicate the spectra of the reference  
502 materials,  $\text{Na}_2\text{AsO}_3$  [As(III)],  $\text{NaHAsO}_4$  [As(V)], orpiment ( $\text{As}_2\text{S}_3$ ) and arsenopyrite ( $\text{FeAsS}$ ). Linear  
503 combination fittings from the spectra of the reference materials for the soils are shown as solid lines.

504

505 Fig. 3 Relationship of the percent decrease in dissolved arsenic (As) and phosphorus (P) in soil B<sub>1</sub>  
506 incubated with the Fe materials. SSS, SCS, RIM, cFH and cZVI denote spent steel shot, fine spent  
507 casting sand, residual iron materials of steel shot production, commercial ferrihydrite and commercial  
508 zero-valent iron, respectively. The regression line is for the by-product Fe materials (SSS, SCS, RIM-  
509 1 and RIM-2), and \*\*\* indicates significance at  $P < 0.001$ . The percent decrease in dissolved As and  
510 P was calculated using Eq. 1.

511

512 Table 1 Selected physico-chemical properties of the soil samples

513

514 Table 2 Elemental and mineralogical composition of the iron materials

515

516 Table 3 Time course of the concentrations of arsenic (As), silica (Si) and phosphorus (P) in soil solution

517 and two-way analysis of variance (ANOVA)

Table 1 Selected physico-chemical properties of the soil samples

Soil sample	pH (H <sub>2</sub> O)	TC (g kg <sup>-1</sup> )	TN (g kg <sup>-1</sup> )	Clay (g kg <sup>-1</sup> )	Selective extraction (g kg <sup>-1</sup> )				HCl-As (mg kg <sup>-1</sup> )
					Fe <sub>d</sub>	Al <sub>o</sub>	Fe <sub>o</sub>	Si <sub>o</sub>	
Soil A	5.18	14.3	1.22	170	9.13	2.77	5.47	0.36	2.80
Soil B <sub>1</sub>	6.54	16.3	1.58	349	19.1	1.60	10.5	0.70	5.83
Soil B <sub>2</sub> <sup>†</sup>	5.99	17.7	1.74	359	17.8	1.59	10.1	0.52	8.36

TC, Total carbon; TN, Total nitrogen; HCl-As, arsenic extractable in 1 mol L<sup>-1</sup> hydrochloric acid

Subscripts “o” and “d” denote oxalate- and dithionite-citrate-extractable elements, respectively.

<sup>†</sup> Data from Suda et al. (2015)

Table 2 Elemental and mineralogical composition of the iron materials

Fe material	Elemental concentration					Mineral	
	Fe (g kg <sup>-1</sup> )	Si (g kg <sup>-1</sup> )	Mn (g kg <sup>-1</sup> )	As (mg kg <sup>-1</sup> )	P (mg kg <sup>-1</sup> )	Major	Minor
SSS	864±43	50.2±15.2	6.22±0.09	37.5±4.1	592±4	Z	Q
SCS	56.4±13.0	355±1	1.48±0.11	3.27±0.47	102±1	Q	Z
RIM-1	590±13	59.8±1.6	50.5±0.9	3.77±0.86	380±14	W, M	H
RIM-2	642±18	57.4±2.2	49.3±1.9	19.5±4.4	406±16	W, M	Z
cFH	532±3	10.8±4.2	2.10±0.04	3.41±0.90	239±4	F	
cZVI	982±4	15.9±0.4	48.4±0.3	76.8±0.7	639±21	Z	

SSS, spent steel shot; SCS, fine spent casting sand; RIM, residual Fe materials of steel shot production;

cFH, commercial ferrihydrite; cZVI, commercial zero-valent iron

Fe, iron; Si, silicon; Mn, manganese; As, arsenic; P, phosphorus

Z, zero-valent iron; Q, quartz; W, wüstite; M, magnetite and/or maghemite; H, hematite; F, ferrihydrite

Table 3 Time course of the concentrations of arsenic (As), silica (Si) and phosphorus (P) in soil solution and two-way analysis of variance (ANOVA)

Sample	Approximate incubation time (days)					
	Soil A			Soil B <sub>1</sub>		
	20	60	100	20	60	100
<b>Dissolved As (<math>\mu\text{g L}^{-1}</math>)</b>						
Control	21.9±2.1 a	108±2 a	98.2±13.3 a	367±11 a	649±32 a	817±7 a
SSS	22.2±0.7 a	6.65±0.20 b	4.38±0.24 b	232±1 b	214±16 b	102±12 b
SCS	22.0±2.6 a	75.8±3.1 c	54.7±2.9 c	344±8 c	598±4 a	660±24 c
RIM-1	13.4±0.2 b	9.21±0.51 b	6.54±0.44 b	323±5 c	454±27 c	397±18 d
RIM-2	24.4±1.0 a	14.8±1.4 d	6.77±0.27 b	323±14 c	443±19 c	353±12 e
cFH	9.32±0.16 c	23.1±0.4 e	41.6±3.9 d	112±4 d	321±3 d	505±15 f
cZVI	2.67±0.36 d	1.57±0.02 f	2.53±0.35 b	72.9±5.7 e	11.1±0.9 e	5.36±0.17 g
<i>Two-way ANOVA</i>						
Fe material ( <i>F</i> )		$P < 0.001$			$P < 0.001$	
Incubation time ( <i>T</i> )		$P < 0.001$			$P < 0.001$	
<i>F</i> × <i>T</i>		$P < 0.001$			$P < 0.001$	
<b>Dissolved Si (<math>\text{mg L}^{-1}</math>)</b>						
Control	8.02±0.10 a	11.3±0.1 a	12.5±0.1 a	11.1±0.2 a	12.0±0.1 ab	13.2±0.1 a
SSS	8.82±0.09 b	12.0±0.2 b	12.5±0.2 a	10.6±0.2 b	11.7±0.1 b	12.5±0.2 b
SCS	8.49±0.02 c	11.8±0.2 b	13.1±0.0 b	11.1±0.1 ab	12.1±0.0 a	13.4±0.1 a
RIM-1	10.8±0.1 d	13.3±0.1 c	14.1±0.1 c	11.2±0.2 a	12.1±0.3 a	13.4±0.1 a
RIM-2	10.1±0.1 e	13.0±0.0 c	13.7±0.0 d	10.9±0.0 ab	12.0±0.1 ab	13.3±0.2 a
cFH	6.07±0.07 f	9.06±0.10 d	11.8±0.3 e	9.11±0.02 c	10.6±0.2 c	12.0±0.1 c
cZVI	8.38±0.10 c	10.1±0.1 e	11.3±0.1 f	10.1±0.2 d	10.6±0.0 c	11.0±0.1 d
<i>Two-way ANOVA</i>						
Fe material ( <i>F</i> )		$P < 0.001$			$P < 0.001$	
Incubation time ( <i>T</i> )		$P < 0.001$			$P < 0.001$	
<i>F</i> × <i>T</i>		$P < 0.001$			$P < 0.001$	
<b>Dissolved P (<math>\text{mg L}^{-1}</math>)</b>						
Control	1.15±0.03 a	2.01±0.01 ab	2.24±0.03 a	0.480±0.013 a	0.597±0.005 a	0.667±0.013 a
SSS	1.44±0.01 b	1.96±0.04 b	1.18±0.02 b	0.448±0.027 ab	0.579±0.034 a	0.561±0.016 b
SCS	1.17±0.02 a	2.02±0.02 ab	2.27±0.02 a	0.482±0.006 a	0.601±0.011 a	0.654±0.019 a
RIM-1	1.15±0.01 a	2.05±0.03 a	2.26±0.01 a	0.474±0.013 a	0.576±0.002 a	0.629±0.010 ac
RIM-2	1.20±0.02 c	1.99±0.02 ab	1.98±0.10 c	0.466±0.030 a	0.570±0.012 ab	0.604±0.017 c
cFH	0.435±0.01 d	1.03±0.02 c	1.27±0.14 b	0.259±0.000 c	0.359±0.012 c	0.459±0.012 d
cZVI	1.60±0.02 e	0.413±0.020 d	0.313±0.024 d	0.402±0.010 b	0.475±0.004 d	0.416±0.010 e
<i>Two-way ANOVA</i>						
Fe material ( <i>F</i> )		$P < 0.001$			$P < 0.001$	
Incubation time ( <i>T</i> )		$P < 0.001$			$P < 0.001$	
<i>F</i> × <i>T</i>		$P < 0.001$			$P < 0.001$	

SSS, spent steel shot; SCS, fine spent casting sand; RIM, residual iron material of steel shot production; cFH, commercial ferrihydrite; cZVI, commercial zero-valent iron. Values followed by the same letter within a column are not significant ( $P = 0.05$ , Tukey's test).



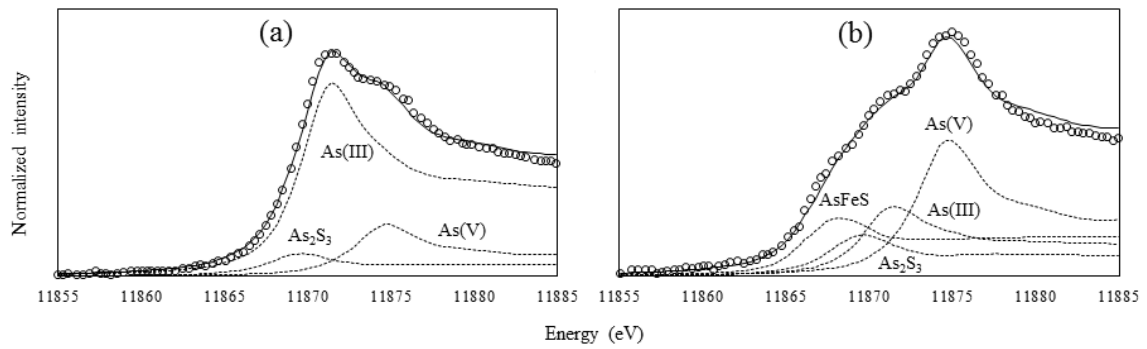


Fig. 2 Arsenic K-edge XANES spectra of solid phases of (a) the control for soil B2 and (b) soil B2 incubated with commercial zero-valent iron. Broken lines indicate the spectra of the reference materials,  $\text{Na}_2\text{AsO}_3$  [As(III)],  $\text{NaHAsO}_4$  [As(V)], orpiment ( $\text{As}_2\text{S}_3$ ) and arsenopyrite ( $\text{FeAsS}$ ). Linear combination fittings from the spectra of the reference materials for the soils are shown as solid lines.

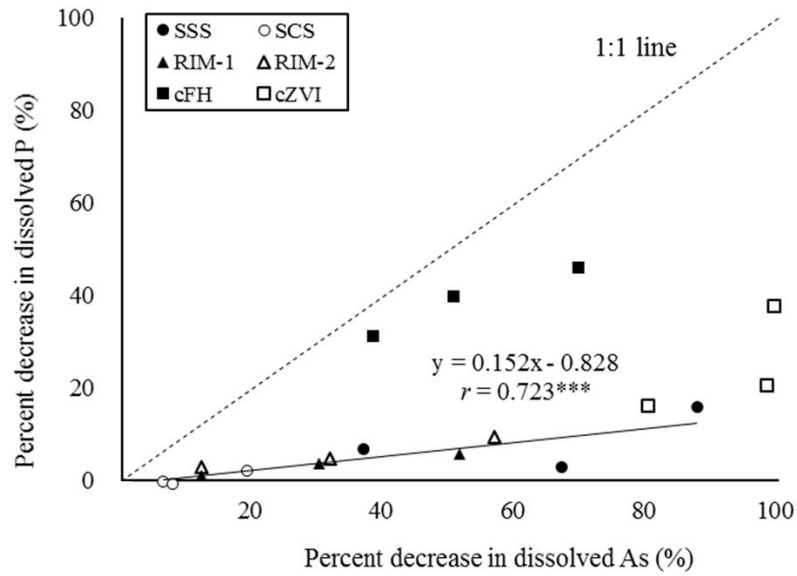


Fig. 3 Relationship of the percent decrease in dissolved arsenic (As) and phosphorus (P) in soil B<sub>1</sub> incubated with the Fe materials. SSS, SCS, RIM, cFH and cZVI denote spent steel shot, fine spent casting sand, residual iron materials of steel shot production, commercial ferrihydrite and commercial zero-valent iron, respectively. The regression line is for the by-product Fe materials (SSS, SCS, RIM-1 and RIM-2), and \*\*\* indicates significance at  $P < 0.001$ . The percent decrease in dissolved As and P was calculated using Eq. 1.